triply reduced species. There are, however, indications that the Cu(I) dianion gives a better fit to the optical spectrum than the trianion. The strongest evidence in support of the Cu(I) dianion is that $\Delta E_{1/2}^{2-3}$ for Cu is less than $\Delta E_{1/2}^{2-3}$ for the free base.

Further evidence that a trianion is not produced comes from the fact that similar complexes of Zn and Pd having closed d shells do not exhibit this third reversible wave. In fact, no conclusive evidence for trianions exists in the porphyrin literature. The only species which are known to be reversibly formed with charges of 3- are those in which the charge is delocalized between the metal and the porphyrin ring, as in the case of $[PFe^{I}]^{3-}$ and $[PCo^{I}]^{3-}$. Thus, the best alternative is the formation of a Cu(I) dianion. It is interesting to note that the potential for this reaction, Cu(II) $\rightleftarrows$ Cu(I), would be the most negative ever observed for reduction at the metal center of a copper complex, which is usually reduced in the range of +1 V to -0.7 V.

Acknowledgment. The support of the National Science Foundation (K.M.K., Grant No. CHE 79 21536), the Robert A. Welch Foundation (K.M.K., Grant E-680), and the Division of Chemical Sciences, U.S. Department of Energy (L.K.H.), under Contract DE-AC0276 CH 00016 is gratefully acknowledged. The authors wish to thank Dr. J. J. Andrē for aid in the ESR measurements and Dr. Jack Fajer for several helpful discussions.

Registry No. $(CN)_4(TPP)Cu$, 54329-88-3; (TPP)Cu, 14172-91-9; $[(CN)_4(TPP)Cu^{II}]^-$, 80471-07-4; $[(CN)_4(TPP)Cu^{II}]^{2-}$, 80471-08-5; $[(CN)_4(TPP)Cu^{I}]^{3-}$, 80471-09-6.

Contribution from the Molecular Theory Laboratory, The Rockefeller University, Palo Alto, California 94304, the Molecular Research Institute, Palo Alto, California 94304, and the Extraterrestrial Research Division, NASA-Ames Research Center, Moffett Field, California 94035

Interaction of Metal Ions and Nucleotides: Possible Mechanisms for the Adsorption of Nucleotides on Homoionic Bentonite Clays

PETER LIEBMANN, GILDA LOEW,* STANLEY BURT, JAMES LAWLESS, and R. D. MacELROY

Received April 21, 1981

In this study we have used a recently formulated INDO-type semiempirical molecular orbital method to characterize the binding of 5'-AMP, 5'-IMP, 5'-GMP, 2'-AMP, and 3'-AMP to hydrated Zn^{2+} and Mg^{2+}, a process presumed to occur when they are adsorbed in the interlamellar space of ion-exchanged homoionic bentonite cays. The energetics of complex formation and modes of cation-nucleotide binding obtained appear to account for the three types of specificities observed: the preference (1) of Zn^{2+}-exchanged clays for 5'-AMP > 5'-IMP ≥ 5'-GMP, (2) of Zn^{2+}-exchanged clays for 5'-AMP > 2'-AMP > 3'-AMP, and (3) of 5'-AMP for Zn^{2+} rather than Mg^{2+}-exchanged clays. In addition, Zn^{2+} has been shown to bind to the clay more strongly than Mg^{2+}, in keeping with the observed ability of Zn^{2+} to displace Mg^{2+} from bentonite clay. Also, the preference of Mg^{2+} for phosphate-site binding and of Zn^{2+} for N_7-phosphate bridge binding has been clearly demonstrated for 5'-nucleotides. These results strongly implicate direct cation-nucleotide complex formation in the adsorption of nucleotides on homoionic clays and imply that such complexes could then be involved in subsequent polymerizations.

Background

It has been proposed that the origin of life proceeded by the formation of important biomonomers from simpler molecules such as methane, ammonia, and water, postulated as part of the primitive earth's atmosphere. A good deal of work has been done demonstrating the plausibility of such prebiotic organic syntheses. Much less is known about how the biomonomers were concentrated from dilute aqueous solutions and condensed to biopolymers. One suggestion is that clays or other minerals may have provided a surface onto which small molecules could be concentrated and subsequently polymerized.[1-7] However, most clays do not readily adsorb such important biomonomers as amino acids and nucleotides at the nearly neutral pH which is thought to have existed in the primitive ocean.

Recently it has been demonstrated in experiments at NASA-Ames[8] that metal ions as exchangeable cations in the clays alter this behavior markedly. When naturally occurring Wyoming bentonite clay was converted to a homoionic clay by repeated washing with metal halide solution, the Na^+, Li^+, and K^+ clays, in common with the naturally occurring one, did not adsorb 5'-AMP from dilute solution under prebiotic conditions. However, a variety of other metal dications, when exchanged in the clay, did adsorb nucleotides in the order Zn^{2+} > Cu^{2+} > Ni^{2+} > Co^{2+} > Mg^{2+}. Some of these cations, particularly Zn^{2+}, which produced the most effective nucleotide adsorbing clay, are fundamental to contemporary nucleotide biochemistry. In addition, recent experiments have shown that Zn^{2+} is an efficient and stereospecific catalyst in template-directed polymerization of an activated nucleic acid derivative.[9] These works suggest that metal complexes may also have played an important role in organic chemical evolution on the primitive earth.

Subsequent experiments as NASA-Ames have characterized nucleotide adsorption on homoionic bentonite clays in more detail. Specifically, the pH dependence of adsorption of 5'-AMP on Zn^{2+} bentonite has been determined, and a maximum at about pH 7.4 is observed. Under these conditions, the nucleotide is in dibasic form. Langmuir isotherms were obtained at pH 7.4 for the adsorption of a variety of nucleotides: 5'-AMP, 5'-IMP, 5'-GMP, 5'-ADP, 5'-CMP, 5'-UMP, 2'-

* To whom all correspondence should be addressed at The Rockefeller University.

(1) Bernal, J. D. "The Physical Basis of Life"; Routledge and Kegan Paul: London, 1951.
(2) Lahav, N.; Chang, S. *J. Mol. Evol.* **1976**, *8*, 357.
(3) Theng, B. K. G. "The Chemistry of Clay-Organic Reactions"; Wiley: New York, 1974; pp 274-281.
(4) Paecht-Horowitz, M.; Berger, J.; Katchalsky, A. *Nature (London)* **1970**, *228*, 636.
(5) Paecht-Horowitz, M. *Isr. J. Chem.* **1973**, *11*, 369.
(6) Otroschenko, V. A.; Vasilyeva, N. V. *Origins Life* **1977**, *8*, 25.
(7) Ponnamperuma, C. *Abstr. Int. Clay Conf.* **1969**.
(8) Lawless, J.; Edleson, E. H. "Life Sciences and Space Research"; Pergamon Press: New York, 1980; Vol. VIII, pp 83-88.
(9) Lohrmann, R.; Bridson, P. K.; Orgel, L. E. *Science (Washington, D.C.)* **1980**, *208*, 1464.

0020-1669/82/1321-1586$01.25/0

Table I. Measured Affinity Constants and Fractional Cation Site Availability for Nucleotide Adsorption on Homoionic Bentonite Clays

A. Metal Cation Specificity for Adsorption of 5′-AMP

clay cation	a_s[a]	log K_{clay}[b]	log K_{aq}[c]
Zn^{2+}	0.80	3.18	2.72
Cu^{2+}	0.24	3.12	3.18
Ni^{2+}	0.004	3.16	2.84
Co^{2+}	0.003	2.82	2.56
Mg^{2+}	0.005	2.44	1.97

B. 5′-Nucleotide Specificity for Zn^{2+}-Exchanged Clays

nucleotide	a_s[a]	log K_{clay}[b]	log K_{aq}[c]
5′-AMP	0.80	3.18	2.7
5′-IMP	0.41	2.36	2.6
5′-GMP	0.78	2.20	

C. Nucleotide Isomer Specificity for Zn^{2+}-Exchanged Clays

nucleotide	a_s[a]	log K_{clay}[b]
5′-AMP	0.80	3.18
2′-AMP	0.53	3.05
3′-AMP	0.55	2.91

[a] a_s = number of moles of nucleotide adsorbed at saturation ≡ number of exchangeable cationic sites in clay. [b] With assumption of a 1:1 cation–nucleotide complex. [c] Values taken from ref 27.

AMP, and 3′-AMP on Zn^{2+} bentonite and also to 5′-AMP on a series of homoionic bentonite clays with Zn^{2+}, Cu^{2+}, Ni^{2+}, Co^{2+}, and Mg^{2+} as exchangeable cations. From these isotherms, assuming a 1:1 M^{2+}–nucleotide complex, an association constant and the percent of metal sites in the clay available for complex formation were determined.[8] As summarized in Table I, these properties vary significantly for different nucleotides with the same metal (Zn^{2+}) and for different metals with the same nucleotide (5′-AMP). Neither of these observed variations is well understood.

In this investigation, a number of metal–nucleotide complexes were characterized, with use of semiempirical quantum mechanical methods, with the aim of explaining both nucleotide and cation specificities and providing insight into the nature of the interactions involved in such complex formation.

The two metal cations Zn^{2+} and Mg^{2+}, which were most and least effective in adsorbing 5′-AMP onto homoionic bentonite clays, were chosen in this study to investigate the origin of the observed metal ion specificity. Interactions of Zn^{2+} and five different nucleotides, 5′-AMP, 5′-IMP, 5′-GMP, 2′-AMP, and 3′-AMP, were also included in this study to try to account for the observed specificities of Zn which adsorbs 5′-AMP > 5′-IMP ≥ 5′-GMP and 5′-AMP > 2′-AMP ≥ 3′-AMP.

In addition to model cation–nucleotide complexes, a model for the interaction of the hydrated cations with the homoionic bentonite clay was also studied. Optimum interactions of Zn^{2+} and Mg^{2+} cation with the clay were calculated as a function of metal–silicate oxygen distance. Relative stabilities and electron distributions for the Zn^{2+}- and Mg^{2+}-exchanged clays were obtained and compared to known experimental differences.

The validity of the results obtained in this study can be measured by the extent to which they consistently explain the observed metal ion and nucleotide adsorption specifities. The detailed descriptions obtained in these studies should help elucidate the nature of metal–nucleotide complexes and their role in adsorption of nulceotides onto clay from dilute solutions.

Models and Assumptions

In the experimental study reported, Wyoming bentonite, a dioctahedral, three layer 2:1 silicon/aluminum clay, was used. A representative unit, or tactoid, of this clay is shown schematically in Figure 1. Each platelet consists of three

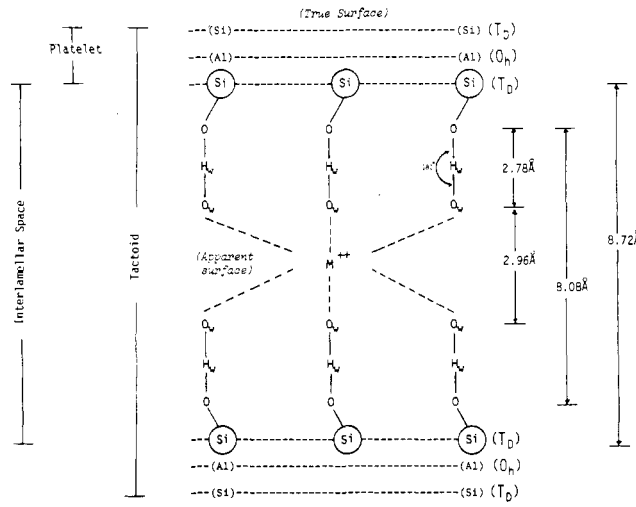

Figure 1. Schematic representation of typical bentonite clay with hydrated cation at postulated exchangeable site between two silicate layers. Distances shown are taken from X-ray structure of Mg^{2+} vermiculite.

layers—two repeating silicate tetrahedral layers alternating with a dioctahedral aluminum layer. There is evidence that the exchangeable cations are on the outer surface and in the interlamellar space between two silicate layers of repeating platelet units of the tactoid. While the extent of hydration of the cation varies with experimental conditions, under the condition of the experiments performed at NASA-Ames the exchangeable cation is most likely fully hydrated. A crystal structure of Mg^{2+}-exchanged homoionic montmorillonite clay yields a hexahydrated Mg^{2+} with a hydration shell of six specific site-bound water molecules, three of which are bound to the upper layer and three of which are bound to the lower layer between which the metal intercalates, as shown in two views in Figure 2.[10] In these studies we have used this crystal structure to represent the cation and the hydration shell of intercalated Zn^{2+} and Mg^{2+} ions.

All of the experiments were performed with RNA-type nucleotides at pH ~7.4 where they would be adsorbed in dibasic form. Figure 3a shows 5′-AMP in this form. For 5′-IMP, we have considered their enol form with an OH group at the position labeled C_6 and for 5′-GMP the more common keto form with a C=O group at that position. The 2′-AMP nucleotide has a phosphate at the 2′-position and a 3′-OH and 5′-OH group; and in the 3′-AMP nucleotide, the phosphate is on the C_3' atom with an OH group on C_2' and C_5'.

Upon adsorption, the nucleotides are thought to form a complex with the exchangeable cation (Figure 1). In these studies, the nucleotide was assumed to replace either one or two H_2O molecules of hydration, depending on the mode of binding to the cation. Further, steric constraints of nucleotide binding to the cation were assumed to force two additional H_2O molecules from the inner-shell hydration sphere, leading to a four-coordinated cation–nucleotide–H_2O complex. Thus cation–nucleotide complex formation was represented by eq 1 where M = metal cation, n = number of cation-bound H_2O molecules in the complex, and ΔE = energy of the reaction.

$$[M{\cdot}6H_2O]^{2+} + \text{nucleotide} \xrightarrow{\Delta E} [M{\cdot}nH_2O{\cdot}\text{nucleotide}] + (6-n)H_2O \quad (1)$$

In the calculation of ΔE, three possible types of metal–nucleotide–H_2O complexes were considered, as shown schematically in Figure 3b–d. In the complex labeled type I, the cation forms a bidentate complex with N_7 of the purine base

(10) Mathieson, A. McL. *Am. Miner.* **1958**, *43*, 216.

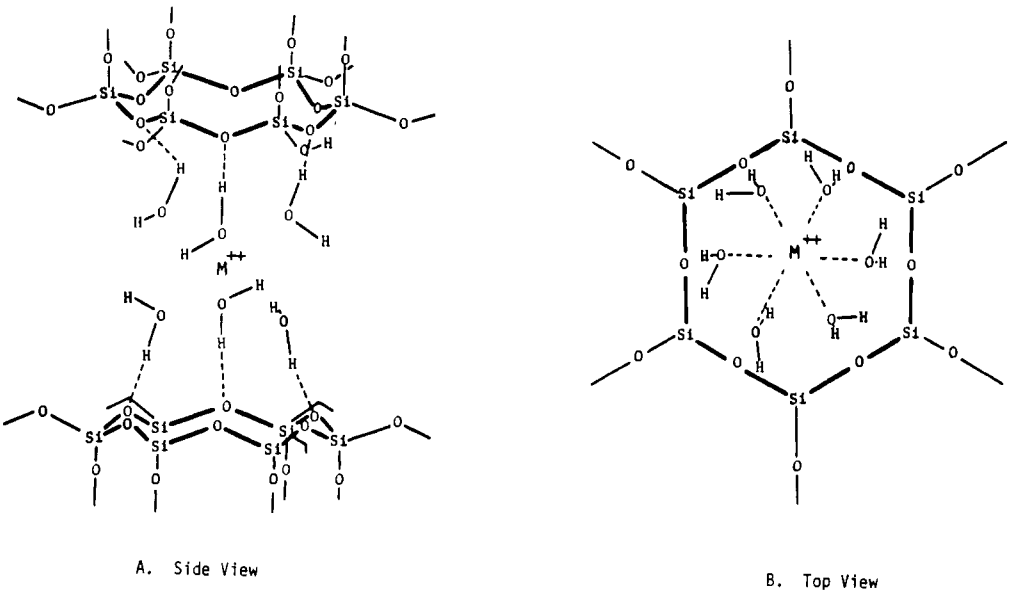

Figure 2. Geometry of a repeating unit of two silicate layers with a hydrated cation intercalated between the layers taken from an X-ray structure of magnesium-containing vermiculite.[10]

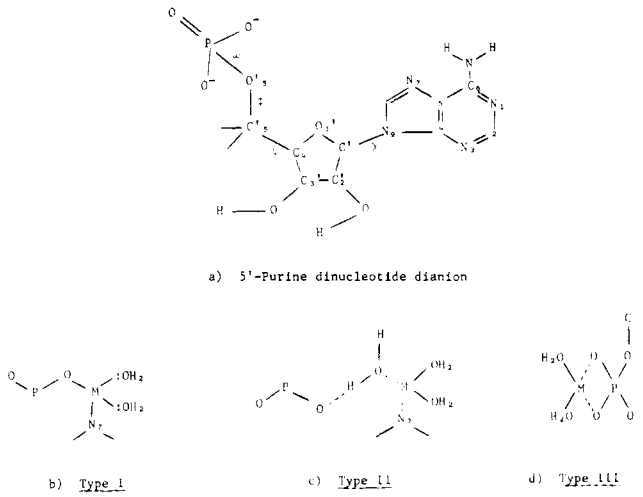

Figure 3. (a) Schematic structure of a typical 5′-purine nucleotide, 5′-AMP, with torsion angles defined. For 5′-GMP the substituents at C_6 is an C=O group, and for 5′-IMP the substituents at C_6 is an OH group. Schematic representation of postulated metal cation binding to mononucleotides (b) type I, (c) type II, and (d) type III.

and one phosphate oxygen atom. In the binding labeled type II, the metal also binds directly to N_7 of the purine base, but only through H_2O to the phosphate oxygen. In both type I and type II complexes, two H_2O's of hydration are retained and additional H-bond interaction of one of these bound H_2O molecules with nearby substituents on the six-membered ring (i.e., NH_2 of adenine, OH of insoine, and the C=O group of guanine) were also considered. N_7 was chosen as the preferred site of cation binding to the base since most X-ray structure determinations of metal–nucleotide binding show the N_7 to be the preferred site of attachment to the base itself.[11]

Both type I and type II bindings are only possible for the 5′-nucleotides since the attachment of the phosphate moiety to the sugar ring in the 2′- and 3′-nucleotides makes it sterically impossible for simultaneous N_7 and phosphate group interactions with the cation even through H_2O. In 2′- and 3′-nucleotides, however, cation binding to N_7 alone is possible, while retaining three H_2O molecules. This mode of binding is also called type II binding for these nucleotides.

In type III complexes (Figure 3d), the metal is presumed to bind symmetrically to two phosphate oxygen atoms of the nucleotide and two H_2O molecules with no other direct interaction. Type III binding is possible for 5′-, 2′-, and 3′-nucleotides and should show the least nucleotide specificity.

Method and Procedure

All-valence electron semiempirical quantum mechanical methods are now available which can be used to characterize nucleotides and their covalent complexes with metal dications. In particular, two such methods have been used in this study. One, called perturbative configuration interaction using localized orbitals (PCILO) was developed specifically in the laboratory of Pullman for conformational analysis of large molecules.[12] It has been used extensively by us[13,14] and other investigators[15] to study nucleotide, peptide, and opiate conformations. This method was used in this study to determine and characterize low-energy conformers of the nucleotides themselves. Another semiempirical method, a new INDO-type (intermediate neglect of differential overlap) method which includes transition metals and total geometry optimization[16] has been used to this study to obtain metal–nucleotide complex energies, geometries, and electronic structures of the three types of model complexes described above.

Input geometries for the nucleotides were taken from an X-ray crystal structure of 5′-AMP-C_2′-ENDO.[17] This structure was used to make starting geometries for 2′-AMP-C_2′-ENDO, 5′-IMP-C_2′-ENDO, and 5′-GMP-C_2′-ENDO isomers with additional X-ray structure data for the different purine bases.[18,19] The starting geometry for 3′-AMP-C_3′-ENDO was obtained from and X-ray structure of 5′-AMP C_3′-ENDO.[20] Except for 3′-AMP-C_3′-ENDO, the C_2′-ENDo

(11) Hodgson, D. J. In "Progress in Inorganic Chemistry"; Lippard, S. J., Ed.; Wiley: New York, 1977; Vol. 23, pp 211–254.
(12) Diner, S.; Malrieu, J. P.; Jordan, F.; Gilliert, M. *Theor. Chim. Acta* **1969**, *15*, 100.
(13) Pack, G. R.; Loew, G. *Biochem. Biophys. Acta* **1978**, *519*, 163.
(14) Loew, G. H.; Burt, S. K. *Proc. Natl. Acad. Sci. U.S.A.* **1978**, *75*, 7.
(15) Pullman, B.; Saran, A. *Prog. Nucleic Acid Res. and Mol. Bio.*, **1976**, *18*, 215.
(16) Zerner, M.; Loew, G. H.; Kirchner, R. F.; Mueller-Westerhoff, U. T. *J. Am. Chem. Soc.* **1980**, *102*, 589.
(17) Neidle, S.; Uhlbrandt, W.; Acharu, A. *Acta. Crystallogr., Sect. B* **1976**, *B32*, 1850.
(18) Rubin, J.; Breenan, T.; Sundaralingam, M. *Science (Washington, D.C.)* **1971**, *174*, 1020.
(19) Rao, S. T.; Sundaralingam *J. Am. Chem. Soc.* **1969**, *91*, 1210.

sugar pucker was the only one considered. The dianionic RNA form of all nucleotides was used (Figure 3), consistent with experimental conditions.

Three types of nucleotide conformations were considered as candidates for binding to the cation when adsorbed onto the clay: (1) the experimental geometry, (2) a PCILO optimized experimental geometry, and (3) the lowest energy conformer obtained by starting with the experimental geometry and by using the PCILO method for energy calculations of nested rotations about χ, ψ, and ϕ (Figure 3a) followed by local geometry optimization. For each of the five nucleotides, these three candidate conformers wereused as input to the INDO-type program and total geometry optimization performed. The energies of the totally optimized nucleotide conformers obtained by the INDO-type method were used to calculate energies of complex formation as given by eq 1.

The energy of the hexaaquo complexes $Zn{\cdot}(H_2O)_6^{2+}$ + $Mg(H_2O)_6^{2+}$, the other reactants in eq 1, were also obtained by total geometry optimization using the same INDO-type method.

Initial geometries for each type of metal–nucleotide complex were selected by imposing an approximately tetrahedral local symmetry about the cation. These starting geometries were then fully optimized with use of the INDO-type program with the theoretical parameterization appropriate for geometry optimization.

Type I complexes, i.e., metal ion binding directly to both N_7 and phosphate oxygen atoms, could be formed with only one of the candidate 5′-nucleotide conformations—the lowest energy PCILO conformer.

Both type II and type III complexes (Figure 3c,d) could be formed by the other two candidate nucleotide conformers considered, i.e., the experimental and PCILO optimized experimental geometries. Final optimized geometries for all metal ion–nucleotide complexes were used in eq 1 to calculate complex stabilities.

So that the relative binding characteristics of Zn^{2+} and Mg^{2+} to montmorillonite clays could be obtained, the clay model shown in Figure 2A,B, consisting of a unit of the silicate layer (i.e., Si_6O_{12} and the hexaaquo cation), was used with coordinates taken from an X-ray structure of Mg^{2+}–vermiculite. In the model unit used in calculations, hydrogen atoms were added to the bridging oxygen atom shown with "dangling bond" in Figure 2B. Energies were calculated for subsequent structures of Mg^{2+} and Zn^{2+} homoionic clays as a function of interlamellar spacing (Figure 1). The minimum energies obtained with each cation binding to the interstitial layer were compared with each other and with the energy of silicate layers of the clay without the cation.

Results and Discussion

The energy of $Zn{\cdot}6H_2O{\cdot}Si_6O_{12}H_6$ model clay complex (Figure 2B) was calculated as a function of $Zn{\cdot}OH_2$ bond length. As shown in Table II, the optimum distance obtained was $R(Zn–OH_2)$ = 1.97 Å, corresponding to an intermolecular O_{Si}–O_{Si}, nucleus to nucleus, spacing of 7.5 Å. The results for the $Mg^{2+}{\cdot}6H_2O{\cdot}Si_6O_{12}H_6$ model clay complex were $R(Mg–OH_2)$ = 1.85 Å and an O_{Si}–O_{Si}, nucleus to nucleus, spacing of 6.7 Å. This model may be viewed as representing the case where crystalline swelling has occurred, and the resulting distances are in agreement with cases where it is known that the interlaminar phase is comprised of a double layer of water.[21-24] As shown in Table II, the Zn clay complex is calculated to be more stable than the Mg–clay complex by 88 kcal/mol. These results are consistent with the observation that Zn^{2+} has a higher affinity than Mg^{2+} in binding the bentonite clay.[24]

Table II. Calculated Energies of Model Clay–Cation–Hydrated Complexes

	E, au	ΔE, kcal/mol	$\Delta(\Delta E)^c$	$R(M–OH_2)$,[d] Å	$R(O_{Si}–O_{Si})$,[d] Å
$Zn{\cdot}6H_2O$·clay	−449.2126	−1112.87[a]	0	1.97	7.5
$Mg{\cdot}6H_2O$·clay	−449.0726	−1024.93[a]	88	1.85	6.7
$[Zn{\cdot}6H_2O]^{2+}$	−110.1347	−828.6[b]	284.2	1.87	
$[Mg{\cdot}6H_2O]^{2+}$	−110.5359	−1080.37[b]	32.5	1.67	
$3H_2O$·clay	−339.0320				
H_2O	−18.1357				

[a] Energy of complex formation calculated from M^{2+} + $3H_2O$ + clay·$3H_2O$ → $[M{\cdot}clay{\cdot}6H_2O]^{2+}$. [b] Energy of hydration calculated from M^{2+} + $6H_2O$ → $[M{\cdot}6H_2O]^{2+}$. [c] $\Delta(\Delta E)$ = stabilization energy of complex relative to that of $Zn{\cdot}6H_2O$·clay. [d] Optimized cation–OH_2 distance and corresponding distance between silicate oxygen atoms in top and bottom layer.

As shown in Table II, the calculated relative stability of the Zn^{2+}- and Mg^{2+}-hydrated complexes is reversed. Mg^{2+} cation is calculated to form a more stable hexaaquo complex than Zn^{2+} cation. Further, we predict that the hexaaquo complex of Zn is stabilized by interaction with the clay, while the hexaaquo complex of Mg^{2+} is destabilized in the clay.

Another important feature of the ion-exchange clays is the electron distribution and, in particular, the extent of electron transfer to the cation from the silicate layers of the clay between which they are intercalated. From Table III, we see that Zn^{2+} acquires 1.25 e in its hydrated complex in the clay, but that most of the electron density (1.2 e) comes from the six waters of hydration and only 0.05 e from the clay. Similar behavior is seen for Mg^{2+}, where 1.11 e are transferred to it in the clay with 1.08 coming from the six waters of hydration and 0.03 e from the clay. The presence of the cation in the clay appears to strengthen the oxygen–silicate bond in the Zn complex and eliminate the weak hydrogen bond between the silicate oxygens and water. The presence of the clay has some effect on the charge distribution in the hydrated cation complex. There is more charge transfer to the metal in the clay, and the metal–water bond is somewhat strengthened.

Table IV gives the calculated energy of totally optimized nucleotide geometries from the INDO-type calculation starting from three different initial geometries: (1) a composite X-ray structure, (2) the X-ray structure "refined" by using the PCILO method, and (3) the lowest energy conformer of the X-ray structure obtained from performing energy calculations for nested rotations and local geometry optimization with the PCILO method. For all nucleotides, the refined geometries were lower in energy than the X-ray structure.

The optimized geometries obtained with these three initial nucleotide conformers are shown in Figure 4a–c for 5′-AMP. Similar geometries were obtained for 5′-IMP and 5′-GMP. Only the conformer of Figure 4a, the lowest energy one, can form a bidentate, type I complex with metal cations. The other two conformers (Figure 4b,c) can form type II and type III complexes.

Tables V–VII give the calculated complex energies for each of the three types of cation–nucleotide complexes considered.

Tables VIII–X give the energy of formation for each complex calculated from eq 1. For type I, II, and III complexes, four, three, and four water molecules, respectively, are assumed to be displaced from the cation hydration shell in the clay (i.e., n = 2, 3, and 2 in eq 1).

Figure 5 shows the final geometry optimized type I, II, and III complexes of 5′-AMP with Zn^{2+}, without H-bonding of the cation bound water to the exocyclic NH_2 group. Similar

(20) Kraut, J.; Jensen, L. H. *Acta Crystallogr.* **1963**, *16*, 79.
(21) McBride, M. B.; Pinnavaia, J. J.; Mortland, M. M. *J. Phys. Chem.* **1975**, *79*, 2430.
(22) Grim, R. E. "Clay Mineralogy"; McGraw-Hill: New York, 1968.
(23) Keren, R.; Shainberg, I. *Clays Clay Miner.* **1979**, *27*, 145–151.
(24) Lawless, J., unpublished data.

Table III. Calculated Electron Distribution in Model Cation–Clay–Hydrated Complexes

	q_M[a]	q_{O_W}[b]	$q_{H_W}^{HB}$[c]	$q_{H_W}^{HB}$[d]	$\Sigma_q H_2O$[e]	ρ_{M-O_W}[f]	ρ_{O-Si}[f]	$\rho_{O_{Si}-H_W}$[f]
$3H_2O$·clay		0.60–	0.34+	0.24+	0		0.480	0.024
Zn·$6H_2O$·clay	0.75+	0.59–	0.41+	0.38+	0.20+	0.34	0.507	0.000
Zn·$6H_2O$	0.90+	0.56–	0.38+	0.36+	0.18+	0.30		
Mg·$6H_2O$·clay	0.89+	0.43–	0.27+	0.33+	0.17+			
Mg·$6H_2O$	1.53+	0.63–	0.34+	0.37+	0.08+			

[a] Net charge on cation calculated from a Mulliken population analysis from INDO-type calculations. [b] Net charge on oxygen atom of water which is hydrogen bonded to silicate oxygen. [c] Net charge on hydrogen atom of water which is hydrogen bonded to silicate oxygen. [d] Net charge on hydrogen atom of water which is *not* hydrogen bonded to silicate oxygen. [e] Net charge on each H_2O molecule. [f] Calculated bond overlap densities which are a measure of bond strength.

Table IV. Calculated Energies of Purine Nucleotides with Totally Optimized Geometries[a]

conformer[b]	5′-AMP[c]	5′-IMP[c]	5′-GMP[c]	2′-AMP[c]	3′-AMP[c]
(1) exptl	−252.0335	−257.7003	−269.0475	−252.0176	−252.0372
(2) exptl $PCILO_{opt}$	−252.0740	−257.7457	−269.0903		
(3) $PCILO_{min}$	−252.2785	−257.9566	−269.2875		

[a] Total optimization with new INDO-type program. Energy in atomic units (1 au = 627.5 kcal/mol). [b] Starting conformations for INDO geometry optimization: (1) X-ray structure; (2) the experimental geometry refined by local geometry optimization by using the PCILO method; (3) a low-energy conformation obtained from nested rotations about torsion angles and local geometry optimization by using the PCILO method (only these conformers can form a type I compound). [c] 5′-AMP, 5′-IMP, 5′-GMP, and 2′-AMP have C_2′-ENDO sugar puckers; 3′-AMP has a C_3′-ENDO pucker.

Table V. Calculated Energies of Optimized Complex of Zn^{2+} and Mg^{2+} with 5′-Purine Nucleotides: Type I, M^{2+} Binds to N_7 and Phosphate Oxygen[a]

	5′-AMP	5′-IMP	5′- GMP
	A. Zn^{2+}		
with H bond[b]	−290.1684	−296.0579	−307.4438
without H bond	−290.5121	−296.1835	−307.4967
	B. Mg^+		
with H bond		−296.1178	−307.3659
without H bond	−290.4271		

[a] Energy in au of fully optimized complex by INDO method. Metal cation forms a four-coordinated tetrahedral (T_d) complex bound to N_7, O phosphate, and two H_2O molecules. Complexes formed with a INDO fully optimized nucleotide conformer obtained from a low-energy conformer from the PCILO method by nested rotations and local geometry optimization. [b] Complex with H bond between H_2O and O_6 of guanine, OH of inosine, and NH_2 of adenine. Complex energy is worse because this H bond is formed at the expense of the direct M^{2+}–O phosphate interaction.

Table VI. Calculated Energies of Optimized Complexes of Zn^{2+} and Mg^{2+} with Purine Nucleotides: Type II, M^+ Binds to N_7 and through H_2O to Phosphate Oxygen[a]

	exptl nucleotide geometry[b]		$PCILO_{opt}$ exptl geometry[c]	
	no H bond	H bond	no H bond	H bond
		A. Zn^{2+}		
5′-AMP	−308.3569	−308.3786	−308.4288	−308.2508
5′-IMP	−313.9197	−313.8612	−314.0799	−313.9905
5′-GMP	−325.1482	−325.2191	−325.4545	−325.4024
2′-AMP	−308.1002			
3′-AMP	−308.0300			
		B. Mg^{2+}		
5′-AMP	−308.5464	−308.5600	−308.5796	−308.4066
5′-IMP		−313.9971		
5′-GMP				

[a] Energy (au) of fully optimized complex by the INDO method. Metal cation forms a four-coordinated T_d complex to N_7 and three waters of hydration. In the 5′-nucleotides, but not the 2′- and 3′-nucleotides, one of these bound H_2O molecules can hydrogen bond to the phosphate group. [b] Cation complexes formed with an INDO totally optimized nucleotide obtained by starting with the experimental geometry. [c] Cation complexes formed with an INDO totally optimized nucleotide geometry starting with a PCILO optimized experimental geometry.

complex geometries were found with the other 5′-nucleotides. Figure 6 gives the final geometry optimized complexes for type

Table VII. Calculated Energies of Optimized Complexes of Zn^{2+} and Mg^{2+} with Purine Nucleotides: Type III, M^{2+} Binds to Two Phosphate Oxygen Atoms[a]

	exptl nucleotide geometry[b]	$PCILO_{opt}$ exptl nucleotide geometry[c]
	A. Zn^{2+}	
5′-AMP	−290.1684	−290.1677
5′-IMP	−295.8498	−295.8637
5′-GMP	−307.1798	−307.1885
2′-AMP	−290.1620	
3′-AMP	−290.1606	
	B. Mg^{2+}	
5′-AMP	−290.5078	−290.4980
5′-IMP	−296.1927	
5′-GMP	−307.5312	
2′-AMP	−290.5286	
3′-AMP	−290.5112	

[a] Energy (au) of fully optimized complex by the INDO method. Metal cation forms a four-coordinated complex binding symmetrically to two phosphate oxygen atoms (C_{2v}) and, in addition, to two equivalent H_2O molecules. [b] Cation complex formed with an INDO optimized nucleotide geometry obtained by starting from an experimental nucleotide geometry. [c] Cation complexes obtained with an INDO optimized nucleotide geometry starting with a PCILO optimized experimental geometry.

II and III complexes of 2′-AMP and 3′-AMP with Zn, and for comparison, 5′-AMP results are repeated.

The results summarized in Table VIII show a different complex stability and preferred type of binding of Zn^{2+} to different 5′-purine nucleotides. 5′-AMP and 5′-IMP are predicted to have preferential binding to Zn^{2+} in the type I mode, in which both N_7 and a phosphate oxygen atom bind directly to the cation. 5′-GMP, on the other hand, prefers to bind to Zn^{2+} in a type II mode, directly to N_7 and through a cation-bound H_2O to the phosphate oxygen atom.

In complex formation involving N_7 (type I, II), the hydrated Zn moiety cannot interact simultaneously with the phosphate group and with the nearby exocyclic NH_2, C=O, or OH ring substituent. Such H bonding is made at the expense of the direct (or through H_2O) M^+—O phosphate interaction. None of the 5′-purine nucleotides binds Zn^{2+} preferentially to the phosphate oxygen atoms only (type III). Complexes involving N_7 are preferred independent of the nucleotide geometries used to form the cation complex.

The most stable complex formed by each 5′-nucleotide dianion with Zn^{2+} is given in brackets in Table VIII. Assuming these complexes would be preferentially formed when

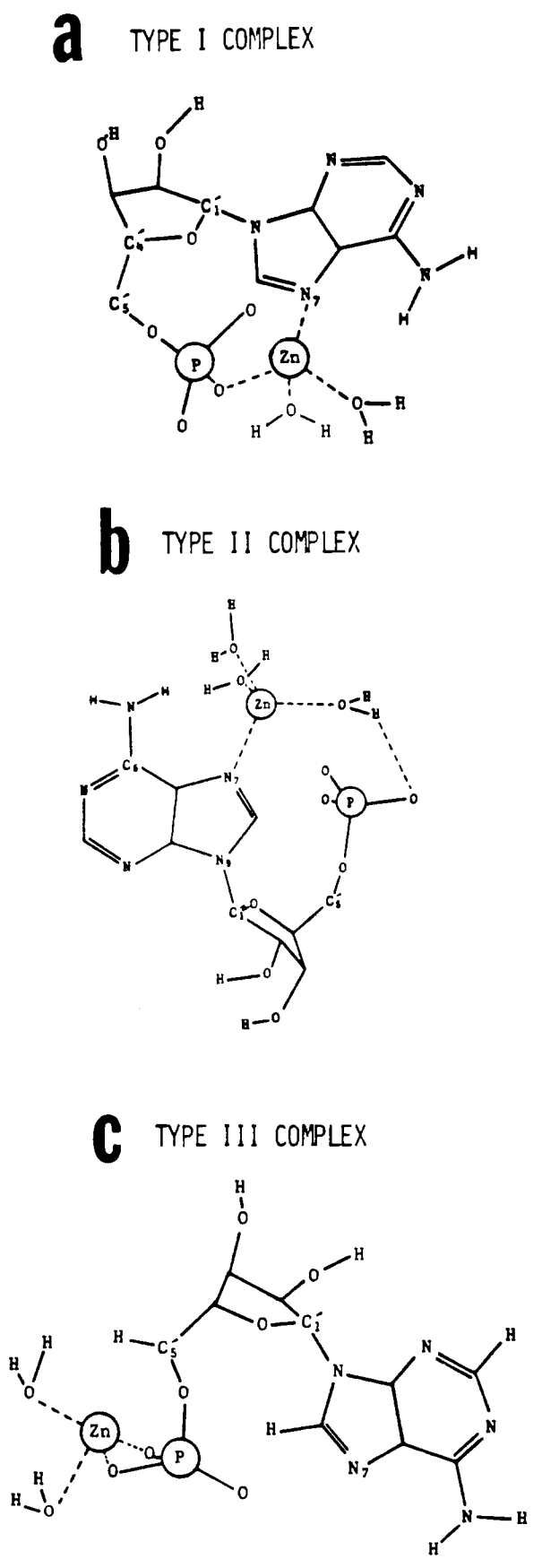

Figure 4. Totally optimized geometry of three different conformers of 5′-AMP. (a) A low-energy conformer obtained from the PCILO method by nested rotations and local geometry optimization with INDO-type wavefunction. (b) Experimental geometry refined by local geometry optimization using the PCILO method and then reoptimized with total geometry optimization, using the INDO-type method. (c) Experimental geometry totally optimized by the INDO-type method.

the nucleotide is adsorbed into a fully hydrated Zn^{2+}-exchanged homoionic bentonite clay, one sees that the calculated order of stability is consistent with the experimentally determined association constants. 5′-AMP forms the most stable complex, while 5′-IMP and 5′-GMP form optimum complexes of approximately equal stability.

Table IX gives differences in stability and preferred type of binding of Zn^{2+} to 5′-, 3′-, and 2′-AMP. We see from this table that both 2′-AMP and 3′-AMP preferentially bind Zn^{2+} at the phosphate group (type III), while for 5′-AMP either kind of binding to N_7 is preferred to binding only to the phosphate oxygen atoms. Comparing the calculated energies of the most stable complex formed by each nucleotide, we see that Zn is predicted to form complexes in order of decreasing stability (5′-AMP > 2′-AMP > 3′-AMP), again consistent with measured association constants for these nucleotides adsorbed on Zn^{2+}-exchanged homoionic bentonite clays.

In addition to the nucleotide specificity demonstrated by Zn^{2+}-exchanged clays, our results can also account for the preferential adsorption of 5′-AMP by Zn^{2+} rather than Mg^{2+}-exchanged clays. As shown in Table X, Mg–5′AMP complexes are all less stable than the corresponding Zn–5′-AMP complexes. Moreover, Mg^{2+} binds preferentially to the phosphate oxygen atoms (type III binding), while, as previously states, Zn^{2+} preferentially forms a bridging complex with a phosphate oxygen atom and N_7 of the purine base. The calculated differences in stability and of mode of binding are consistent with the observation that Mg–nucleotide complexes are generally observed to bind to the phosphate group only, while Zn^{2+} has been shown to bind to different 5′-purine nucleotides at both the N_7 and phosphate oxygens.[25]

It is of interest to examine the charge distributions in these complexes and their possible relation to relative stabilities. While the exchangeable cations have a formal charge of 2+ as shown in Table XI, when they form hexaaquo complexes there is a net charge transfer of 1.1 e to the Zn and 0.47 e to the Mg from the six H_2O molecules. When nucleotides are adsorbed and bind to the cation displacing all but two or three H_2O molecules, there is a net increase in electrons transferred to the cation in all types of complexes studied. In Zn^{2+} complexes there are 1.4–1.5 e transferred to the Zn^{2+} and in Mg^{2+} complexes, 1.0–1.1 e to the Mg^{2+}, with the additional electron transfer coming mainly from the phosphate oxygens. Thus Zn^{2+}, which forms the more stable nucleotide complex, also has more electrons transferred to it than Mg^{2+}. By contrast, for the hexaaquo Zn^{2+} and Mg^{2+} complexes, the Mg^{2+} forms the more stable complex, with less electrons transferred to it. These results suggest that charge-transfer (i.e., covalent) interactions would be more important in the metal cation–nucleotide complexes and electrostatic (ionic) interactions more important in the metal cation–hydration complexes.

In addition to elucidating the origin of nucleotide specificities, some insight into the possible origins of relative cation-site availability to 5′-, 2′-, and 3′-nucleotides is also provided by these calculations. The type I complexes preferred by 5′-AMP, as well as the type II complexes shown in Figure 6a, have a maximum lateral dimension of 8.6 Å. As shown in Figure 6b, these complexes are much less extended than the type III complexes formed by the 2′- and 3′-nucleotides. Exchangeable cation sites in the clays have been estimated to be separated by approximately 10 Å.[26] Type III binding, then, of the nucleotide at one cationic site could interfere with nearest-neighbor binding of another nucleotide and reduce site

(25) Tu, A. T.; Hiller, M. J. "Metal Ions in Biological Systems"; Sigel, H., Ed.; Marcel Dekker: New York, 1974; Vol. 1, pp 1–4.
(26) Van Olphen, H. "An Introduction of Clay Colloid Chemistry", 2nd ed.; Wiley: New York, 1977; pp 254–255.
(27) Smith, R. M.; Martell, A. E. "Critical Stability Constants"; Plenum Press: New York, 1975; Vol. 2, pp 266–289.

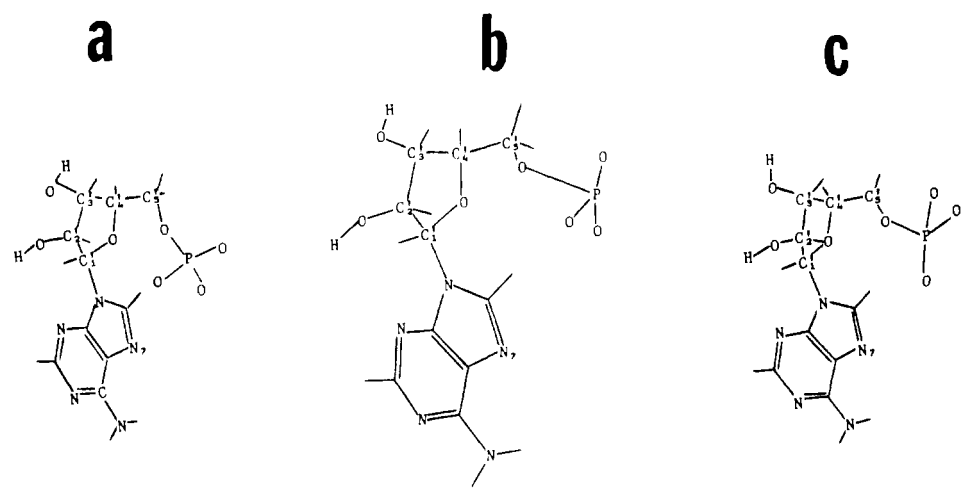

Figure 5. Three types of metal–nucleotide complexes found with 5′-purine nucleotides totally optimized geometries obtained by the INDO-type method. (a) Type I complex: metal cation forms four-coordinated tetrahedral bidentate complex with N_7 and phosphate oxygen atom of nucleotide and two H_2O molecules. (b) Type II complex: metal cation forms a four-coordinated tetrahedral complex by binding directly only a N_7 and through H_2O to a phosphate oxygen. (c) Type III complex: metal cation forms a four-coordinated complex binding only to two phosphate oxygen atoms of the nucleotide with no interaction with the purine base.

Table VIII. Calculated Stabilities of Different Types of Complexes of Zn with 5′-Purine Nucleotides[a,b]

$$Zn{\cdot}6H_2O + \text{Nucleotide} \xrightarrow{\Delta E} \text{Nucleotide}{\cdot}Zn{\cdot}nH_2O + (6-n){\cdot}H_2O$$

	type I		type II				type III			
			exptl nucleotide		$PCILO_{opt}$		exptl nucleotide	$PCILO_{opt}$	log K_a	a_s
	no H bond	H bond[c]	no H bond	H bond[c]	no H bond	H bond[c]				
5′-AMP	[−403]	−187	−374	−387	−394	−282	−341	−315	3.18	0.80
5′-IMP	[−398]	−320	−309	−272	−381	−325	−347	−330	2.36	0.41
5′-GMP	−387	−354	−234	−379	[−399]	−367	−339	−318	2.20	0.80

[a] All ΔE are in kcal/mol. [b] Preferred interactions are denoted by brackets. [c] H-bonding interaction between H_2O bound to cation and substituent at the C_6 position of the six-membered ring.

Table IX. Calculated Stabilities (ΔE, kcal/mol) of Different Types of 5′-AMP, 3′-AMP, and 2′-AMP Complexes

$$Zn{\cdot}6H_2O + \text{Nucleotide} \xrightarrow{\Delta E} \text{Nucleotide}{\cdot}Zn{\cdot}nH_2O + (6-n){\cdot}H_2O$$

	type I[a]	type II[b]	type III[b]	log K_a	a_s
5′-AMP	[403][c]	387	341	3.18	0.80
2′-AMP		223	[347]	3.05	0.53
3′-AMP		167	[334]	2.91	0.55

[a] Most stable type I complex corresponding to no H bonding of H_2O to NH_2 of adenine. [b] Complexes formed with INDO optimized experimental nucleotide geometries. [c] Preferred interactions are denoted by brackets.

availability to half, which is that observed for 2′- and 3′-AMP. Such an argument, however, only partially accounts for the disparity between Mg^{2+} and Zn^{2+} site availability and does not account for the behavior of 5′-IMP. It is possible, as has been suggested for inosine, that 5′-IMP forms a 2:1 metal nucleotide complex to some extent at the experimental pH of 7.2. The disparity between Zn^{2+} and Mg^{2+} site availability appears to be related to the greater mutual perturbation of the Mg^{2+} by the clay and requires more detailed modeling of the interaction for further elucidation.

Figure 7 shows a geometry optimized Zn–5′-AMP type II complex intercalated into the interlamellar spacing between the two silicate layers of a clay. The geometry of the complex was taken from its optimized coordinates and the geometry of the clay from the X-ray coordinates of vermiculite,[10] with Zn^{2+} placed at the site of the exchangeable cation. Figure 7a shows the Zn-5′-AMP complex in the clay retaining the six waters of hydration originally surrounding the cation before nucleotide adsorption. Calculated interatomic distances indicate that three of these water molecules are sterically crowded site, as indicated in this figure by not showing bonding to the Zn. Removal of these three H_2O molecules leads to the 4-coordinated complex shown in Figure 7b, which we have used as the basis for all calculated energies of complex for-

Table X. Calculated Stabilities (ΔE, kcal/mol) of Zn^{2+} and Mg^{2+} Complexes with 5′-AMP

$$M{\cdot}6H_2O + \text{Nucleotide} \xrightarrow{\Delta E} \text{Nucleotide}{\cdot}M{\cdot}nH_2O + (6-n)H_2O$$

	type I	type II		type III		log K_a	a_s
		exptl[a]	$PCILO_{opt}$[b]	exptl[a]	$PCILO_{opt}$[b]		
Zn(5′-AMP)	[403][c]	387	394	341	315	3.18	0.80
Mg(5′-AMP)	98	25	236	[302]	270	2.44	0.0047

[a] Most stable type II complex formed with INDO optimized experimental nucleotide geometry. [b] Most stable type II complex formed with INDO optimized, PCILO refined, experimental nucleotide geometry. [c] Preferred interactions are denoted by brackets.

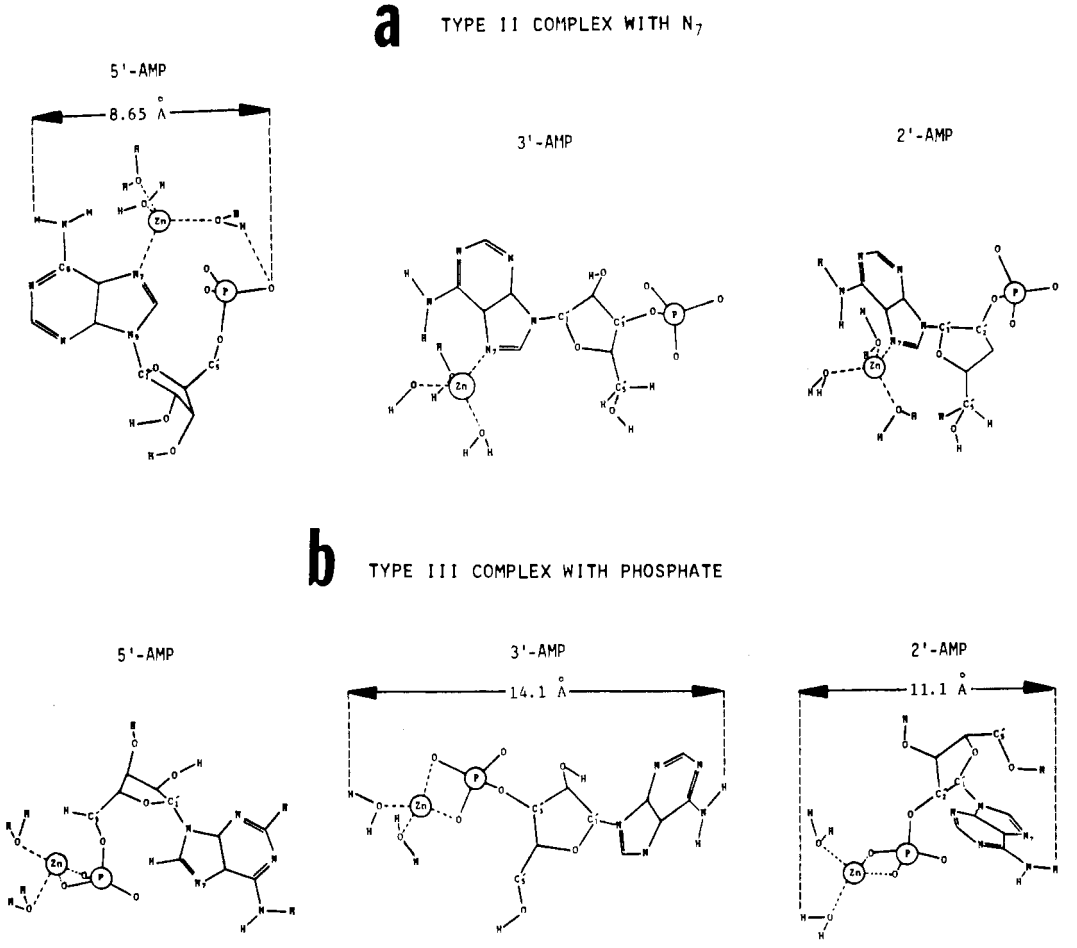

Figure 6. Two types of metal–nucleotide complexes formed with 2′- and 3′-nucleotides totally optimized geometries obtained by the INDO-type method. (a) Type II complex: the cation binds directly to N_7 of the purine base. (b) Type III complex: the cation binds directly to two phosphate oxygen atoms. Also shown for comparison are the results for 5′-AMP and the distance of maximum extension for these types of complexes.

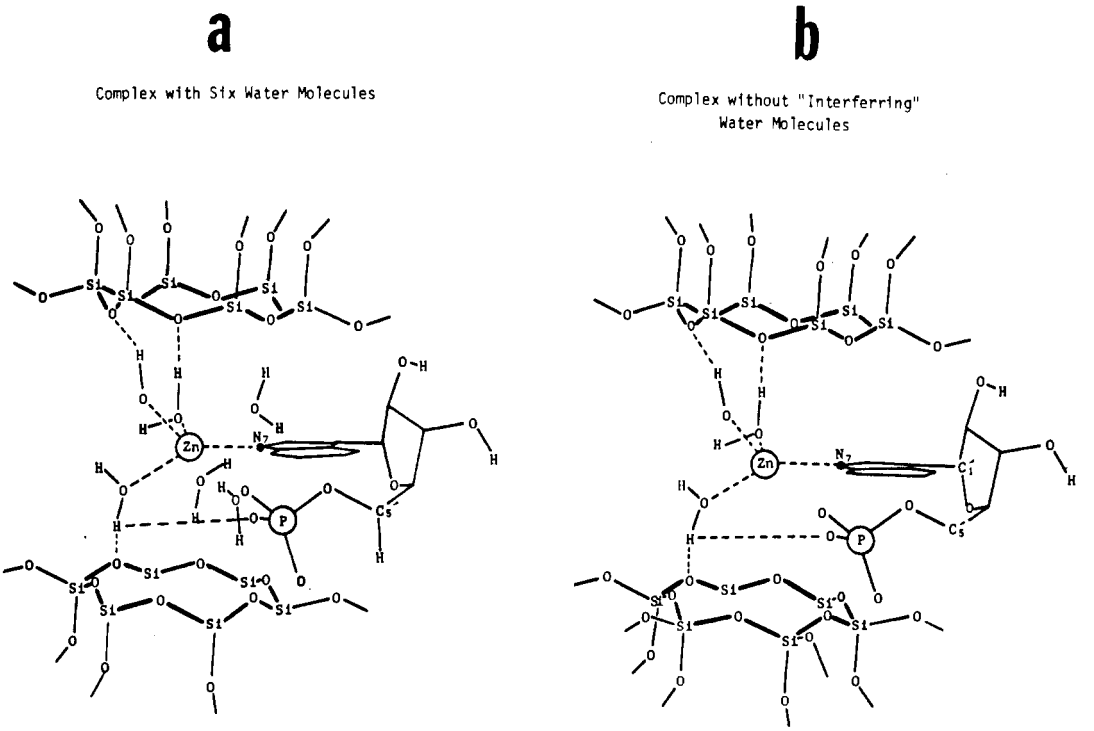

Figure 7. Computer graphic representation of 5′-AMP complexing to the metal cation in the interlamellar space of the clay. The geometry of the silicate layers and the hydrated cation was taken from an X-ray structure of Mg–vermiculite[10] and of the metal nucleotide complex from the total optimized type II complex. (a) Complex with a fully hydrated clay, i.e., with the six water molecules of hydration as in X-ray structure. (b) Four-coordinated complex with three interferring water molecules removed.

Table XI. Net Atomic Charges on Cations and Ligands in Cation-Clay-Hydration Complexes

	M	O_W[a]	O_W[b]	O_p[-c]	N_7
Zn^{2+}	2.0+				
5′-AMP				0.68–	0.28–
$Zn{\cdot}6H_2O$	0.90+		0.56–		
Zn·5′-AMP					
type I	0.53+		0.47–	0.47–	0.41–
type II	0.59+	0.59–	0.50–	0.55–	0.26–
type III	0.61+		0.47–	0.48–	0.25–
Mg^{2+}	2.0+				
5′-AMP				0.68–	0.28–
$Mg{\cdot}6H_2O$	1.53+		0.63–		
Mg·5′-AMP					
type II	0.90+	0.70–	0.54–	0.55–	0.38–
type III	0.91+		0.51–	0.61–	0.26–

[a] H_2O bound to cation and to phosphate oxygen. [b] H_2O bound to cation. [c] Phosphate oxygen bound to cation.

mation. Thus, steric considerations appear to favor the formation of 4-coordinated, rather than 6-coordinated, metal-nucleotide-water complexes in the clay, consistent with the model of complex formation (eq 1) used in this study.

Conclusion

In this study we have characterized the binding of 5′-AMP, 5′-IMP, 5′-GMP, 2′-AMP, and 3′-AMP to hydrated Zn^{2+} and Mg^{2+}, a process presumed to occur when they are adsorbed in the interlamellar space of ion-exchanged homionic bentonite clays. The energetics of complex formation and modes of cation-nucleotide binding obtained appear to account for the three types of specificities observed: the preference (1) of Zn^{2+}-exchanged clays for 5′-AMP > 5′-IMP ≥ ′-GMP, (2) of Zn^{2+}-exchanged clays for 5′-AMP > 2′-AMP > 3′-AMP, and (3) of 5′-AMP for Zn^{2+}- rather than Mg^{2+}-exchanged clays. In addition, Zn^{2+} has been shown to bind to the clay more strongly than Mg^{2+}, in keeping with the observed ability of Zn^{2+} to displace Mg^{2+} from bentonite clay. Also, the preference of Mg^{2+} for phosphate-site binding and of Zn^{2+} for N_7-phosphate bridge binding has been clearly demonstrated for 5′-nucleotides. Finally, differences in mode of binding of Zn^{2+} to different nucleotides and of Mg^{2+} and Zn^{2+} for 5′-AMP could account for some, but not all, of the differences in availability of exchangeable sites of nucleotide binding. These results strongly implicate direct cation-nucleotide complex formation in the adsorption of nucleotides on homionic clays and imply that such complexes could then be involved in subsequent polymerizations.

Acknowledgment. Support for this work by a NASA-Ames Consortium Agreement, No. NCA2-OR630-901, is gratefully acknowledged.

Registry No. 5′-AMP, 61-19-8; 5′-IMP, 131-99-7; 5′-GMP, 85-32-5; 2′-AMP, 130-49-4; 3′-AMP, 84-21-9; Zn, 7440-66-6; Mg, 7439-95-4.

Contribution from the Department of Chemistry, Faculty of Science, Kyushu University 33, Hakozaki, Higashiku, Fukuoka 812, Japan

Noncovalent Interactions in Metal Complexes. 3.[1] Stereoselectivity Caused by Interligand, Hydrophobic CH···π Interaction in 1-*l*-Menthoxy-3-benzoylacetonato Complexes

HISASHI OKAWA,* KOHICHI UEDA, and SIGEO KIDA

Received December 17, 1980

Bivalent and trivalent metal complexes of 1-*l*-menthoxy-3-benzoylacetone (H(*l*-moba)) have been synthesized and characterized by means of NMR, electronic absorption, and circular dichroism spectra. On the basis of the NMR spectrum, it was demonstrated that the cis isomer was preferentially formed in the case of [Co(*l*-moba)$_3$]. CD spectra revealed that [Co(*l*-moba)$_3$] was almost optically pure without any effort for resolution, while [Cr(*l*-moba)$_3$] was partly resolved. [Mn(*l*-moba)$_3$] was also shown to be optically active. The absolute configurations of [Co(*l*-moba)$_3$] and [Cr(*l*-moba)$_3$] were determined to be of the Δ form, the same configuration being supposed for [Mn(*l*-moba)$_3$]. Selective syntheses of the cis-Δ isomer for [M(*l*-moba)$_3$] have been interpreted in terms of the interligand, hydrophobic CH···π interaction operating between the phenyl and the chiral *l*-menthyl groups.

Introduction

Hydrophobic interactions are known to occur in biomolecules and to contribute to forming a distinct structural conformation, which provides the specificity required in most biological processes.[2] Such hydrophobic interactions occur between two aliphatic (or alicyclic) groups, between two aromatic groups, and between aliphatic and aromatic groups. In the cases of metal complexes of low molecular weight, interligand hydrophobic interactions may provide distinct features in stability, structure, and reactivity.[1,3,4] Stability enhancement of ternary complexes owing to hydrophobic ring-ring stacking has been well documented by Sigel and co-workers.[3] Recently, Fisher and Sigel showed that the interligand interaction operating between aromatic and aliphatic groups increases the stability of the ternary complexes containing an amino acid and bipyridyl or *o*-phenanthroline.[4] However, recognition of interligand, hydrophobic interaction in metal complexes has been restricted mostly to stability, and there has been very few applications of this effect to selective syntheses and reactions.[5]

In the preceding papers[1,5] we have shown that in the cobalt(III) complexes with Schiff bases derived from *l*-menthyl β-(2-hydroxybenzoyl)propionate and amino acids, the hydrophobic CH···π interaction between the aromatic ring and the chiral *l*-menthyl group induces an asymmetry around the metal ion (the term "hydrophobic CH···π interaction" will be adopted to describe the interaction operating between an aromatic ring and an alkyl or an alicyclic group). By the use of these optically active complexes, partial asymmetric transformations of racemic amino acids to give one optical isomer were achieved.[5] Thus, interligand, hydrophobic interactions can be applicable for selective syntheses of geo-

(1) Part 2: H. Okawa, Y. Numata, A. Mio, and S. Kida, *Bull. Chem. Soc. Jpn.*, **53**, 2248 (1980).
(2) E. Frieden, *J. Chem. Educ.*, **52**, 754 (1975).
(3) P. R. Mitchell, B. Prijis, and H. Sigel, *Helv. Chim. Acta*, **62**, 1723 (1979) and references therein.
(4) E. Fischer and H. Sigel, *J. Am. Chem. Soc.*, **102**, 2998 (1980).
(5) Y. Numata, H. Okawa, and S. Kida, *Chem. Lett.*, 293 (1979).

0020-1669/82/1321-1594$01.25/0